Defensive shimmering responses in the giant honeybee *Apis dorsata* are triggered by dark stimuli moving against a bright background

Sajesh Vijayan[1]*, Eric J Warrant[2] and Hema Somanathan[1]
1: IISER TVM Centre for Research and Education in Ecology and Evolution (ICREEE), School of Biology, Indian Institute of Science Education and Research Thiruvananthapuram, Kerala, INDIA
2: Lund Vision Group, Department of Biology, University of Lund, Sölvegatan 35, Lund, S-22362 Sweden

ORCID-ID: SV, 0000-0002-5110-1536; EJW, 0000-0001-7480-7016; HS, 0000-0002-4803-3894

Keywords
collective behaviour, defensive behaviour, predator-prey interaction, visual ecology

Abstract

Due to the absence of physical barriers, the open-nesting giant honeybee *Apis dorsata* has evolved a spectacular collective defence behaviour – known as "shimmering" – against predators, which is characterised by travelling waves generated by individual bees flipping their abdomens in a coordinated and sequential manner across the bee curtain. We examined if shimmering is visually-mediated by presenting moving stimuli of varying sizes and contrasts to the background (dark or light) in bright and dim ambient light conditions. Shimmering was strongest under bright ambient light, and its strength declined in dim-light. *A. dorsata* shimmered only when presented with the darkest stimulus against a light background, but not when this condition was reversed (light stimulus against dark background). We suggest that this is an effective anti-predatory strategy in open-nesting *A. dorsata* colonies, exposed to high ambient light, as flying predators are more easily detected when they appear as dark moving objects against a bright sky. Moreover, the stimulus detection threshold (smallest visual angular size) is much smaller in this anti-predatory context (1.6° - 3.4°) than in the context of foraging (5.7°), indicating that ecological context affects visual detection threshold.

Introduction

Honeybee colonies consist of several thousand individuals and brood cells, as well as abundant stores of honey and pollen that must be guarded from predators [1,2]. The giant honeybee *Apis dorsata* is a tropical open-nesting species found on cliff faces, tall trees or man-made structures like water tanks and window ledges [3–7]. Honeybees exhibit a wide array of anti-predatory behaviours [2,8,9], and shimmering behaviour in *A. dorsata* is the first line of defence against aerial flying predators such as hornets which are major predators of honeybees [10]. This behaviour is characterised by a dark travelling wave on the comb surface, and can precede a more aggressive collective stinging response [9,11,10,12].

Shimmering arises from 'flickering' behaviour, a form of dorsoventral abdomen-flipping that occurs stochastically in *A. dorsata* [13]. Once initiated at trigger centres on the bee curtain [14,15], the shimmering wave follows the path of the flying intruder [15]. More trigger centres can form if the intruder persists, as quiescent bees from other regions on the comb initiate shimmering, leading to progressively stronger and larger displays [13]. The waves also accelerate at a few trigger centres that detect approaching waves from further away [16,17]. Shimmering confuses potential predators, and serves as a multi-modal alerting signal for nestmates using mechanoreceptive cues [10], low-frequency comb vibrations [18], or by the release of Nasonov pheromone during wave generation [19].

We used artificial moving stimuli that simulate aerial predators to examine the precise relationships between the visual features of the stimuli and the initiation and strength of shimmering, by varying the relative contrast and visual angles subtended by the stimuli on the bee's eye at different ambient light levels.

We predicted that the strength of shimmering will increase: (1) with an increasing contrast between object and background, (2) for larger stimuli and (3) at higher ambient light levels.

Methods

Experimental set up

The experiments were conducted in October - December 2020 using a natural *A. dorsata* colony consisting of a single comb (1 m width, 1.2 m height; see Supp. Video), hanging from a roof rafter (2 m above the ground) on the IISER Thiruvananthapuram campus, India (8.68°N, 77.14°E).

The stimuli used in this study were made from circular cardboard cut-outs that varied in shade (light-grey, dark-grey or black) and size (diameter: 4, 8 or 16 cm; visual angle subtended: 1.6°, 3.3° and 6.5°, respectively). These were moved either vertically or horizontally by the experimenter standing behind a frame using a string, and relative contrasts were changed by placing them against either a grey or a black background covering the frame (Fig. 1A, Supp. Methods). A trial lasted 15 s and consisted of the stimulus moving 15 times from one side to the other against the front of the frame. The movement was timed to a metronome set to 60 beats per minute to maintain a constant velocity of 1 m/s (40°/s in the visual field of a bee). The experimental control constituted of moving only the string without a stimulus.

The reflectance spectra of the stimuli and backgrounds were obtained using a spectrophotometer (Supp. Methods) and the contrasts of the stimuli against the background were quantified using Weber contrast [20]

$$C_{Weber} = \frac{Intensity_{object} - Intensity_{background}}{Intensity_{background}}.$$

The light-grey, dark-grey and black stimuli had contrasts of 16.4, 6.6 and 0, respectively, against the black background, and 2.4, 0.5 and -0.8, respectively, against the grey background. The effect of ambient light intensity on shimmering was examined by moving the largest black stimulus against the grey background under twilight conditions at dawn and dusk, and the responses were compared to shimmering elicited in bright daylight. The shimmering response of the colony was video-recorded, and the light intensities during trials were sampled using a portable luxmeter.

Quantification of shimmering

A shimmering response is characterised by a distinct ascending phase, a climax and a descending phase [17], of which only the area of the climax stage was considered. Videos were converted to AVI format using FFMPEG (at 25 fps) and analysed frame-by-frame using ImageJ [21]. The overall strength S_{trial} of shimmering in a trial was quantified as

$$S_{trial} = \frac{\sum_{i=1}^{n} S_R}{n_{mov}}$$

where $S_R = Area_{climax} / Area_{hive}$ for the i_{th} climax event, and n_{mov} is the number of times the stimulus was moved in a trial (fixed at 15 per trial). In other words, S_{trial} denotes the average proportion of the hive that shimmered when the stimulus moved once.

Statistical analyses

We compared the strength of shimmering (S_{trial}) in relation to stimulus shade, size and background. Since the values of S_{trial} belong to the interval [0,1], interactions were modelled using beta regression with the date of the trial as a random effect [21]. The panel against which the stimuli were presented (left/right) and the direction of motion (vertical/horizontal) were excluded as the model could not fit all the variables and the irrelevant ones were excluded. We compared shimmering response against the excluded variables using

pairwise comparisons with Bonferroni correction and found no significant differences (Fig. S2), thus justifying their exclusion.

Since the beta probability distribution is defined in the open interval (0,1), and 86% of the trials elicited no shimmering (S_{trial}=0), we rescaled S_{trial} in the dataset using the following equation:

$$x_i^o = \frac{x_i(n-1)+0.5}{n}$$

where x_i is the observed value, n is the number of trials (799 in total) and x_i^o is the rescaled value for that observation. All analyses were carried out in R version 3.6.3 [22], and the beta regression analyses were done using the *betareg* package [23] along with bias correction [24]. We compared four models against the null model: a beta regression model with single precision (ϕ) across all variables (Model 1), a beta regression model with ϕ allowed to vary across stimulus shade and size (Model 2) and a beta regression model with variable ϕ across stimulus shade and size and a bias correction to account for any over-estimation of ϕ (Model 3), and a mixed-effects model with the date of trial as the random effect. The best performing model was chosen on the basis of the Aikake Information Criterion (AIC) (see Table S1).

Further, we estimated the difference in S_{trial} between daylight (n=26) and twilight trials (n=25). The dataset used for the daylight condition is a subset of the data used in the previous analysis with the largest black stimulus against the grey background. Since sample sizes differed between the daylight and twilight groups, we used a bootstrap analysis (10000 iterations) which measured the difference in shimmering response and confidence intervals between the two groups using a paired Student's t-test. The outputs of the bootstrap (estimated difference and confidence interval) were compared to the result of a Student's t-test (independent samples).

Results

A. dorsata shimmers strongly to a dark object moving against a light background

Shimmering responses were only observed in trials where the black stimulus was moved against the grey background (Fig. 1B). Shimmering was strongest with the largest black stimulus (subtending a visual angle of 6.5°), while the intermediate-sized black stimulus (3.3°) resulted in a weaker response and the smallest stimulus (1.6°) did not elicit shimmering (Fig. 1B). Thus, the detection threshold for a moving dark object is likely between 1.6° and 3.3°. Amongst the three beta-regression models, the model with variable precision estimates (Model 2) best explained the data (Table S1, Fig. S3, S4). The distinct behavioural responses and the contrasts of the stimuli (Fig. S1) suggest that bees can distinguish and respond to the stimuli on the basis of contrast and size, leading to strong shimmering responses as the visual angle subtended by the intruding object/predator increases in the visual field of the bees.

Shimmering response in dim-light is less pronounced

Out of the 25 twilight trials carried out during dawn and dusk with the 16 cm black stimulus against the grey background, 13 did not elicit shimmering (illuminance between 0.1-4 lux), and the rest showed varying strengths of shimmering (illuminance between 0.1-45 lux). The mean strength of shimmering during bright daylight conditions (0.261 ± 0.111) was an order of magnitude higher than the response in twilight (0.022 ± 0.038) (Fig. 2A). The difference in S_{trial} between the two groups when estimated using bootstrapping (0.240, 95% CI: [0.177, 0.302]) was almost identical to the difference obtained using a Student's t-test (0.240, 95% CI: [0.192, 0.287], $t_{30.923}$=10.36, $p < 0.0001$) (Fig. 2B).

Discussion

Defence behaviour in honeybees involves several sensory modalities [2], and shimmering is predominantly mediated by visual cues [10,15]. When we simulated predator movement using artificial stimuli, the strongest shimmering responses were obtained only in bright ambient light when the stimulus was darker than

the background. This is unlike the role of contrast in the context of foraging (in *A. mellifera*), where the stimulus can be either brighter or darker than the background and yet elicit similar responses [25]. We also found that the strength of shimmering decreased as stimulus size reduced and resulted in no response with the smallest stimulus.

Detection of dark objects moving against bright backgrounds (e.g. the sky) has been reported in several insects including bees, although mostly in the context of mate-detection or predation [26,27]. Male carpenter bees (*Xylocopa tenuiscapa*) detect and chase inanimate projectiles, mistaking them to be potential mates or rivals, when these objects subtend very small visual angles between 0.4° and 1° (which darken the visual field of a single ommatidium by as little as 2%) [28]. *A. mellifera* drones fly towards moving objects as small as 0.4° across (which darkens the visual field by just 8%) [29]. *A. mellifera* workers can also detect a small black stimulus (0.6°x0.6°) moving at 65°/s against a white background [30], which is significantly smaller than their detection threshold during foraging (3.7°-5°) [31]. Anatomical estimates from the compound eyes of *A. dorsata* suggest coarser visual resolution compared to other honeybees [32], which agrees with recent estimates of detection thresholds in *A. dorsata* in the context of foraging (achromatic: 5.7°, chromatic: 12.4°, Balamurali et al. *in prep*).

Our experiments suggest that *A. dorsata* shimmers in response to dark objects moving against a bright background that subtend a visual angle of at least 3.3° (and likely even smaller, between 1.6° and 3.3°) which is smaller than their achromatic detection threshold while foraging. Using a conservative detection threshold for shimmering of 3.3°, and assuming that a colony shimmers to a hornet which is ~2.3-2.7 cm in length [33], the detection-distance threshold corresponds to ~40-47 cm, which agrees with results from real-world interactions involving free-flying hornets near *A. dorsata* colonies [34].

Open-nesting honeybees such as *A. dorsata* are likely to perceive flying predators as dark objects moving against the bright sky. Hornets are major predators of *A. dorsata* hives [9,18], and *Vespa tropica* (the greater banded hornet) is a common predator in our study location [35]. Moreover, hornets can act as strong evolutionary drivers in the formation of specialised anti-predatory responses in honeybees [36–41]. Shimmering resembles the anti-hornet 'I-see-you' display found in the sympatric cavity-nesting *A. cerana* in which guard bees at the entrance shake their abdomens in a to-and-fro motion in the presence of hornets, which supposedly warns the predator that the bees have detected its presence [37]. Simulating this with black discs resulted in strong abdomen-shaking responses in *A. cerana* to stimuli of size 8° moving at 140°/s ([42] as cited in [2]), which agrees with the achromatic visual detection threshold in *A. cerana* (7.7°) [43].

Although in our study we found that the shimmering response increased with larger stimulus size up to our maximum target size of 6.5°, we cannot rule out the possibility that the response increases further for even larger targets, or simply saturates. Beyond a certain size threshold (which is between 6.5° (current study) and 9.5° [44]), the colony responds to the object with stinging attacks [44], which resembles the defensive response of *A. dorsata* against much larger predators such as birds [11]. The findings from our study using moving objects are consistent with the notion that the shimmering behaviour of the giant honeybee is a response to an aerial predator moving in front of the hive against a bright sky background.

Acknowledgements

SV was funded by the Council for Scientific and Industrial Research, India, SV and HS were funded by IISER Thiruvananthapuram and EJW was funded by the Swedish Research Council (2016-04014). We also thank GS Balamurali for his valuable inputs, and PC Anand for helping with the pilot experiments for this study.

References

1. Seeley TD. 1995 *The wisdom of the hive: the social physiology of honey bee colonies*. Cambridge, Mass: Harvard University Press.

2. Fuchs S, Tautz J. 2011 Colony Defence and Natural Enemies. In *Honeybees of Asia* (eds HR Hepburn, SE Radloff), pp. 369–395. Berlin, Heidelberg: Springer Berlin Heidelberg. (doi:10.1007/978-3-642-16422-4_17)
3. Tan NQ, Chinh PH, Thai PH, Mulder V. 1997 Rafter beekeeping with *Apis dorsata:* some factors affecting the occupation of rafters by bees. *J Apicult Res* **36**, 49–54. (doi:10.1080/00218839.1997.11100930)
4. Thomas S, Varghese A, Roy P, Bradbear N, Potts S, Davidar P. 2009 Characteristics of trees used as nest sites by *Apis dorsata* (Hymenoptera, Apidae) in the Nilgiri Biosphere Reserve, India. *J Trop Ecol* **25**, 559–562. (doi:10.1017/S026646740900621X)
5. Roy P *et al.* 2011 Nesting requirements of the rock bee *Apis dorsata* in the Nilgiri Biosphere Reserve, India. *Trop Ecol* **52**, 285–291.
6. Neupane KR, Woyke J, Poudel SM, Zhang S, Yang H, Singh L. 2013 Nesting site preference and behavior of giant honey bee *Apis dorsata*. *Apimondia 2013* **1225**, 41–42. (doi:10.13140/RG.2.1.4840.0407)
7. Misra TK, Pahari S, Murmu S, Raut SK. 2016 Nesting Behaviour of the Giant Honeybees *Apis dorsata* Occurring in Jhargram, West Bengal, India. *Proc Zool Soc* (doi:10.1007/s12595-016-0176-9)
8. Phiancharoen M, Duangphakdee O, Hepburn HR. 2011 Biology of Nesting. In *Honeybees of Asia* (eds HR Hepburn, SE Radloff), pp. 109–131. Berlin, Heidelberg: Springer Berlin Heidelberg. (doi:10.1007/978-3-642-16422-4_6)
9. Seeley TD, Seeley RH, Akratanakul P. 1982 Colony Defense Strategies of the Honeybees in Thailand. *Ecol Monogr* **52**, 43–63. (doi:https://doi.org/10.2307/2937344)
10. Kastberger G, Weihmann F, Hoetzl T. 2011 Self-Assembly Processes in Honeybees: The Phenomenon of Shimmering. In *Honeybees of Asia* (eds HR Hepburn, SE Radloff), pp. 397–443. Berlin, Heidelberg: Springer Berlin Heidelberg. (doi:10.1007/978-3-642-16422-4_18)
11. Kastberger G, Sharma DK. 2000 The predator-prey interaction between blue-bearded bee eaters (*Nyctyornis athertoni* Jardine and Selby 1830) and giant honeybees (*Apis dorsata* Fabricius 1798). *Apidologie* **31**, 727–736. (doi:10.1051/apido:2000157)
12. Wongsiri S, Lekprayoon C, Thapa R, Thirakupt K, Rinderer TE, Sylvester HA, Oldroyd BP, Booncham U. 1997 Comparative biology of *Apis andreniformis* and *Apis florea* in Thailand. *Bee World* **78**, 23–35. (doi:10.1080/0005772X.1997.11099328)
13. Weihmann F, Hoetzl T, Kastberger G. 2012 Training for Defense? From Stochastic Traits to Synchrony in Giant Honey Bees (*Apis dorsata*). *Insects* **3**, 833–856. (doi:10.3390/insects3030833)
14. Schmelzer E, Kastberger G. 2009 'Special agents' trigger social waves in giant honeybees (*Apis dorsata*). *Naturwissenschaften* **96**, 1431–1441. (doi:10.1007/s00114-009-0605-y)
15. Kastberger G, Weihmann F, Hoetzl T. 2010 Complex social waves of giant honeybees provoked by a dummy wasp support the special-agent hypothesis. *Commun. Integr. Biol.* **3**, 179–180. (doi:10.4161/cib.3.2.10809)
16. Kastberger G, Weihmann F, Hoetzl T, Weiss SE, Maurer M, Kranner I. 2012 How to Join a Wave: Decision-Making Processes in Shimmering Behavior of Giant Honeybees (*Apis dorsata*). *PLoS ONE* **7**, e36736. (doi:10.1371/journal.pone.0036736)
17. Kastberger G, Hoetzl T, Maurer M, Kranner I, Weiss S, Weihmann F. 2014 Speeding Up Social Waves. Propagation Mechanisms of Shimmering in Giant Honeybees. *PLoS ONE* **9**, e86315. (doi:10.1371/journal.pone.0086315)
18. Kastberger G, Weihmann F, Hoetzl T. 2013 Social waves in giant honeybees (*Apis dorsata*) elicit nest vibrations. *Naturwissenschaften* **100**, 595–609. (doi:10.1007/s00114-013-1056-z)
19. Kastberger G, Raspotnig G, Biswas S, Winder O. 2010 Evidence of Nasonov Scenting in Colony Defence of the Giant Honeybee *Apis dorsata*. *Ethology* **104**, 27–37. (doi:10.1111/j.1439-0310.1998.tb00027.x)
20. O'Carroll DC, Wiederman SD. 2014 Contrast sensitivity and the detection of moving patterns and features. *Phil. Trans. R. Soc. B* **369**, 20130043. (doi:10.1098/rstb.2013.0043)
21. Douma JC, Weedon JT. 2019 Analysing continuous proportions in ecology and evolution: A practical introduction to beta and Dirichlet regression. *Methods Ecol Evol* **10**, 1412–1430. (doi:10.1111/2041-210X.13234)
22. R Core Team. 2020 *R: A Language and Environment for Statistical Computing*. Vienna, Austria: R Foundation for Statistical Computing. See https://www.R-project.org/.
23. Cribari-Neto F, Zeileis A. 2012 Beta Regression in R. *J. Stat. Soft.* **34**, 1–24.

24. Grün B, Kosmidis I, Zeileis A. 2012 Extended Beta Regression in *R* : Shaken, Stirred, Mixed, and Partitioned. *J. Stat. Soft.* **48**. (doi:10.18637/jss.v048.i11)
25. de Ibarra NH, Vorobyev M, Brandt R, Giurfa M. 2000 Detection of bright and dim colours by honeybees. *J Exp Biol* **203**, 3289–3298.
26. Bergman M, Lessios N, Seymoure BM, Rutowski RL. 2015 Mate detection in a territorial butterfly—the effect of background and luminance contrast. *Behav Ecol* **26**, 851–860. (doi:10.1093/beheco/arv020)
27. Sauseng M, Pabst M-A, Kral K. 2003 The dragonfly *Libellula quadrimaculata* (Odonata: Libellulidae) makes optimal use of the dorsal fovea of the compound eyes during perching. *Eur. J. Entomol.* **100**, 475–479. (doi:10.14411/eje.2003.071)
28. Somanathan H, Borges RM, Warrant EJ, Kelber A. 2017 Visual Adaptations for Mate Detection in the Male Carpenter Bee *Xylocopa tenuiscapa*. *PLOS ONE* **12**, e0168452. (doi:10.1371/journal.pone.0168452)
29. Vallet AM, Coles JA. 1993 The perception of small objects by the drone honeybee. *J Comp Physiol A* **172**, 183–188. (doi:10.1007/BF00189395)
30. Rigosi E, Wiederman SD, O'Carroll DC. 2017 Visual acuity of the honey bee retina and the limits for feature detection. *Sci Rep* **7**. (doi:10.1038/srep45972)
31. Giurfa M, Vorobyev M. 1998 The angular range of achromatic target detection by honey bees. *J Comp Physiol A* **183**, 101–110. (doi:10.1007/s003590050238)
32. Somanathan H, Warrant EJ, Borges RM, Wallen R, Kelber A. 2009 Resolution and sensitivity of the eyes of the Asian honeybees *Apis florea*, *Apis cerana* and *Apis dorsata*. *J Exp Biol* **212**, 2448–2453. (doi:10.1242/jeb.031484)
33. Girish P, Srinivasan G. 2010 Taxonomic studies of hornet wasps (Hymenoptera: Vespidae) *Vespa* Linnaeus of India. *Rec Zool Surv India* **110**, 57–80.
34. Kastberger G, Schmelzer E, Kranner I. 2008 Social Waves in Giant Honeybees Repel Hornets. *PLoS ONE* **3**, e3141. (doi:10.1371/journal.pone.0003141)
35. Balamurali GS, Reshnuraj RS, Johnson J, Kodandaramaiah U, Somanathan H. 2021 Visual associative learning and olfactory preferences of the greater banded hornet, *Vespa tropica*. *Insect. Soc.* **68**, 217–226. (doi:10.1007/s00040-021-00820-w)
36. Papachristoforou A, Rortais A, Zafeiridou G, Theophilidis G, Garnery L, Thrasyvoulou A, Arnold G. 2007 Smothered to death: Hornets asphyxiated by honeybees. *Curr Biol* **17**, R795–R796. (doi:10.1016/j.cub.2007.07.033)
37. Tan K, Wang Z, Chen W, Hu Z, Oldroyd BP. 2013 The 'I see you' prey–predator signal of *Apis cerana* is innate. *Naturwissenschaften* **100**, 245–248. (doi:10.1007/s00114-013-1019-4)
38. Ken T, Hepburn HR, Radloff SE, Yusheng Y, Yiqiu L, Danyin Z, Neumann P. 2005 Heat-balling wasps by honeybees. *Naturwissenschaften* **92**, 492–495. (doi:10.1007/s00114-005-0026-5)
39. Mattila HR, Otis GW, Nguyen LTP, Pham HD, Knight OM, Phan NT. 2020 Honey bees (*Apis cerana*) use animal feces as a tool to defend colonies against group attack by giant hornets (*Vespa soror*). *PLoS ONE* **15**, e0242668. (doi:10.1371/journal.pone.0242668)
40. Mattila HR, Kernen HG, Otis GW, Nguyen LTP, Pham HD, Knight OM, Phan NT. 2021 Giant hornet (*Vespa soror*) attacks trigger frenetic antipredator signalling in honeybee (*Apis cerana*) colonies. *R. Soc. Open Sci.* **8**, 211215. (doi:10.1098/rsos.211215)
41. Cappa F, Cini A, Bortolotti L, Poidatz J, Cervo R. 2021 Hornets and Honey Bees: A Coevolutionary Arms Race between Ancient Adaptations and New Invasive Threats. *Insects* **12**, 1037. (doi:10.3390/insects12111037)
42. Koeniger N, Fuchs S. 1973 Sound production as colony defence in *Apis cerana*. In *Proceedings of 7th International Congress*, *IUSSI*, London.
43. Meena A, Kumar AMV, Balamurali GS, Somanathan H. 2021 Visual detection thresholds in the Asian honeybee, *Apis cerana*. *J Comp Physiol A* **207**, 553–560. (doi:10.1007/s00359-021-01496-0)
44. Koeniger N, Kurze C, Phiancharoen M, Koeniger G. 2017 "Up" or "down" that makes the difference. How giant honeybees (*Apis dorsata*) see the world. *PLOS ONE* **12**, e0185325. (doi:10.1371/journal.pone.0185325)

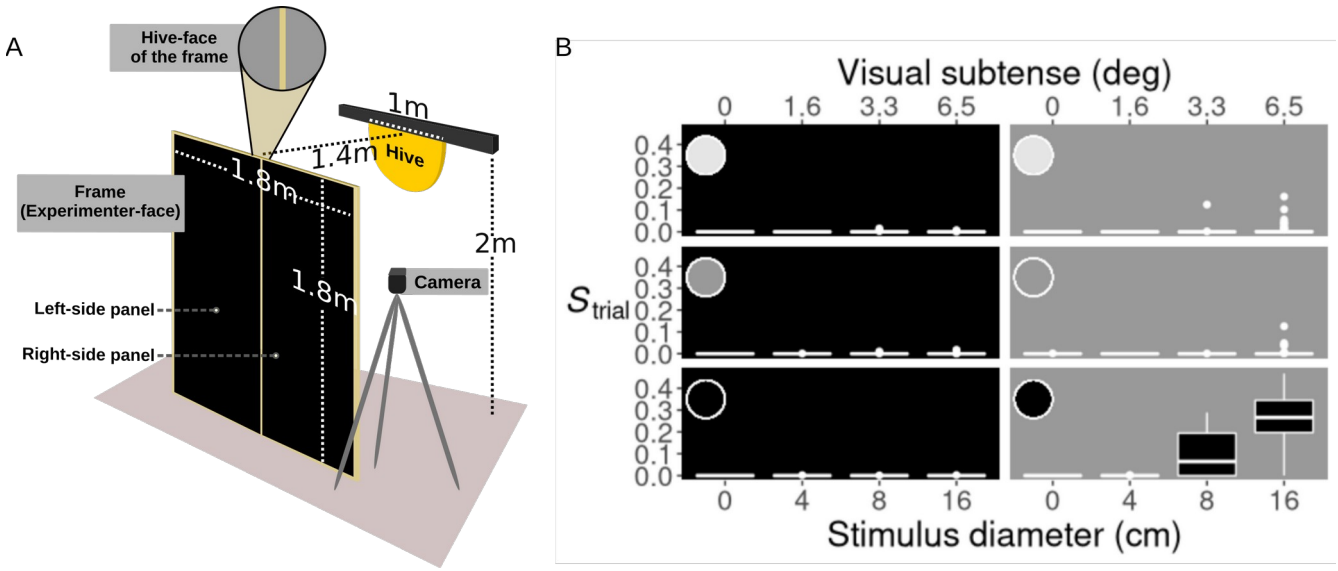

Figure 1. Shimmering responses in *A. dorsata* to moving stimuli (both vertical and horizontal) against dark or light backgrounds. A) Experimental setup. Hive-facing side of the panels were covered with the grey background, while the experimenter-facing side had a black background which could be changed by swivelling the panels. **B)** The relative strength of shimmering (S_{trial}) when presented with moving circular stimuli of varying diameters/visual subtense (x-axes) and shades (light-grey, dark-grey and black (*insets*)) against either a black (*left*) or grey (*right*) background. The *hinges* (horizontal bounds of the box) correspond to the interquartile range (IQR), the *bold horizontal lines* correspond to the medians, the *whiskers* denote the upper/lower hinge ± 1.5xIQR, and the *points* outside the *whiskers* represent outliers.

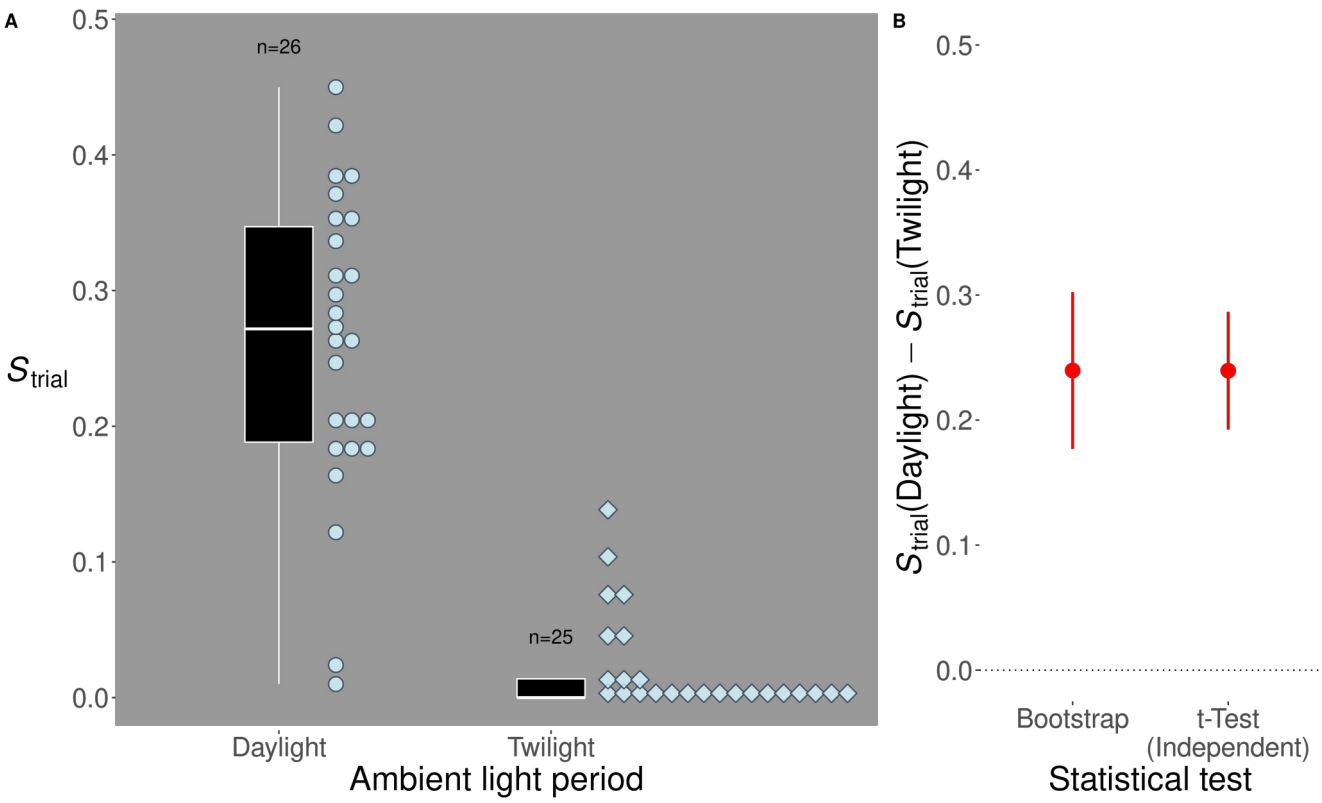

Figure 2. Effect of ambient light on strength of shimmering response, S_{trial}. A) The colony showed only a weak response in twilight (05:55-06:45 h and 18:00-18:50 h; 0.1-45 lux) to the largest black stimulus (diameter 16 cm) when it moved against the grey background. During daylight (07:00-17:00 h; illuminance >1000 lux), the response to the same stimulus-background combination was much more pronounced. The *hinges* (horizontal bounds of the box) correspond to the interquartile range (IQR), the *bold horizontal line* corresponds to the median and the *whiskers* enclose the range of the data. The *blue points* (● daylight, twilight) correspond to the values of S_{trial} binned at intervals of 0.01. **B)** The difference in shimmering strength, S_{trial}, between daylight and twilight conditions estimated using bootstrap and t-test. The *filled circles* are the estimated differences and the *lines* are the 95% confidence intervals.

Supplementary Materials

Defensive shimmering responses in the giant honey bee *Apis dorsata* are triggered by dark stimuli moving against a bright background

Sajesh Vijayan, Eric J. Warrant & Hema Somanathan

Supplementary methods

Experimental setup

The background-frame consisted of two panels that could be swiveled along their vertical axes and the panels were covered with grey and black papers procured locally. The grey stimuli were made using laminated sheets of grey paper manufactured by the Color-Aid Corp. The dark and light grey stimuli were made using Color-Aid Gray-5 and Color-Aid Gray-9 respectively. The black stimulus was made from the same paper as the black background. All stimuli were pasted on to a hard cardboard base to ensure that their shapes remained unchanged over the course of the experiment. Illuminance levels were measured in lux using a Hagner Screenmaster and videos of the trials were recorded using a Sony Handycam HDR CX-405

Reflectance spectra

The reflectance spectra of the stimuli and backgrounds (Fig. S1A) were recorded using an Ocean Insight Ocean-HDX-UV-VIS spectrophotometer connected to an Ocean Optics PX-2 pulsed Xenon light-source. The spectra were captured to a PC (Acer One 110-ICT) running the Ocean View software and saved as a spreadsheet.

Reflectance spectra and contrasts of stimuli

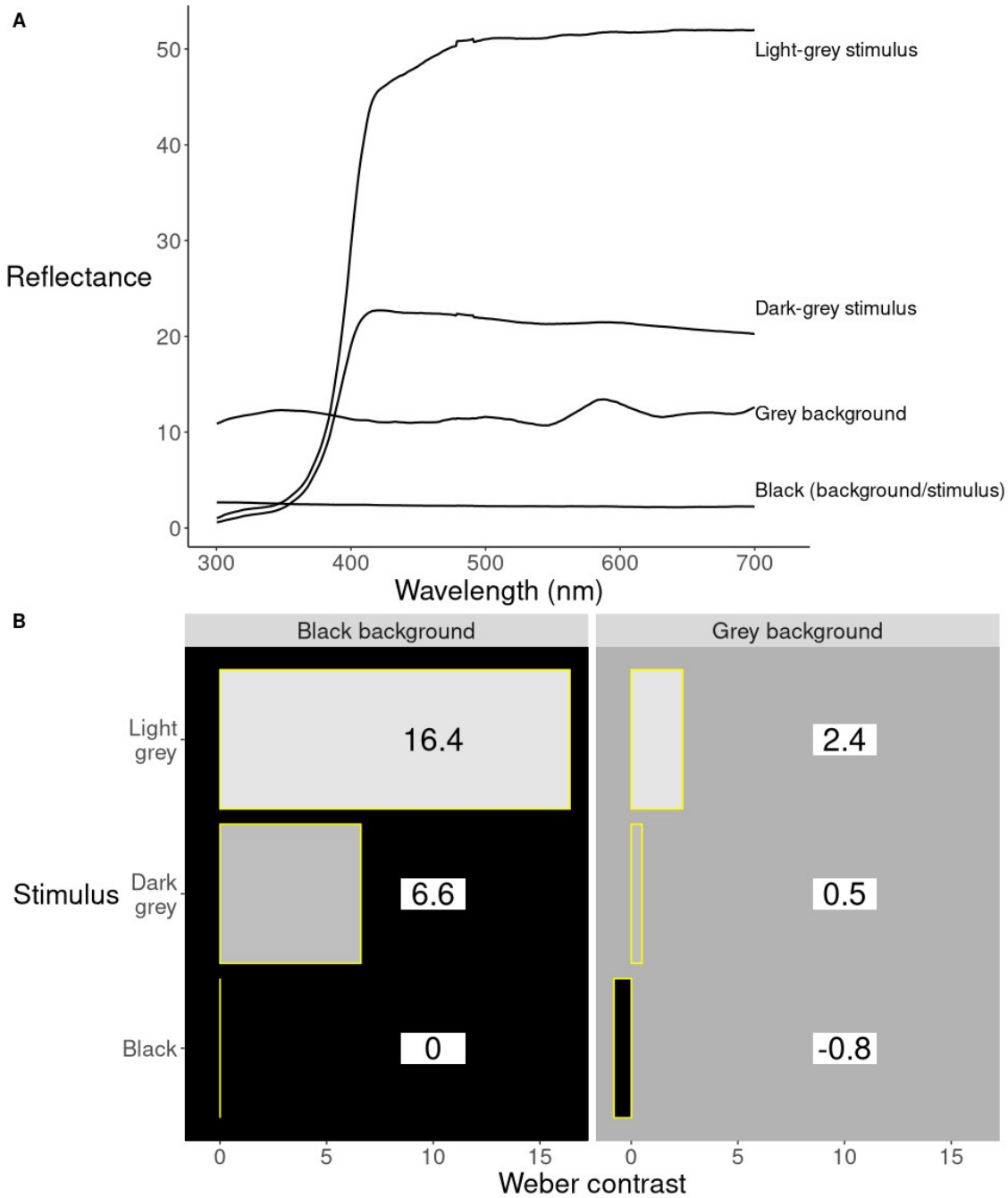

Figure S1. A) Reflectance spectra of the stimuli and backgrounds **B)** The Weber contrasts of the stimuli against the grey or black backgrounds were calculated using the formula provided in the main text, adapted from O'Carroll & Wiederman 2014. The contrast values are written inside/beside the corresponding *bars*.

Supplementary results:

Effect of orientation of motion and side of the trial on shimmering response

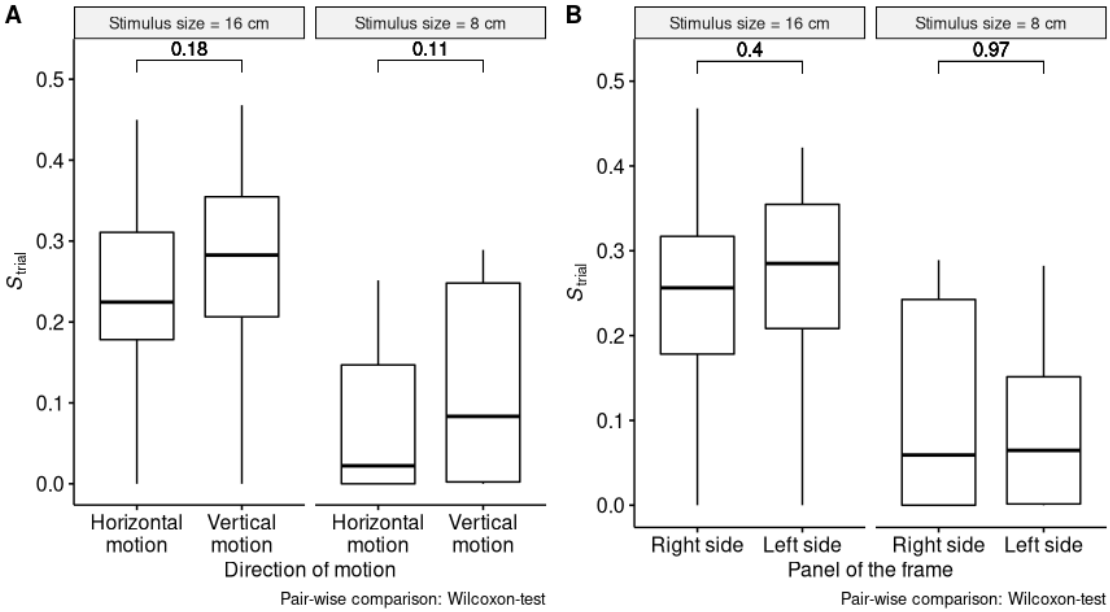

Figure S2. Pairwise comparison of shimmering responses between direction of motion **(A)** and side of the panel **(B)**. S_{trial} refers to the shimmering strength of each trial (refer to main text). The *numbers in boldface* correspond to the p-value of the comparison. There was no effect of direction of motion or side of panel for all stimuli sizes. Hence these two variables were excluded from the final model.

Beta-regression modelling and comparison between models

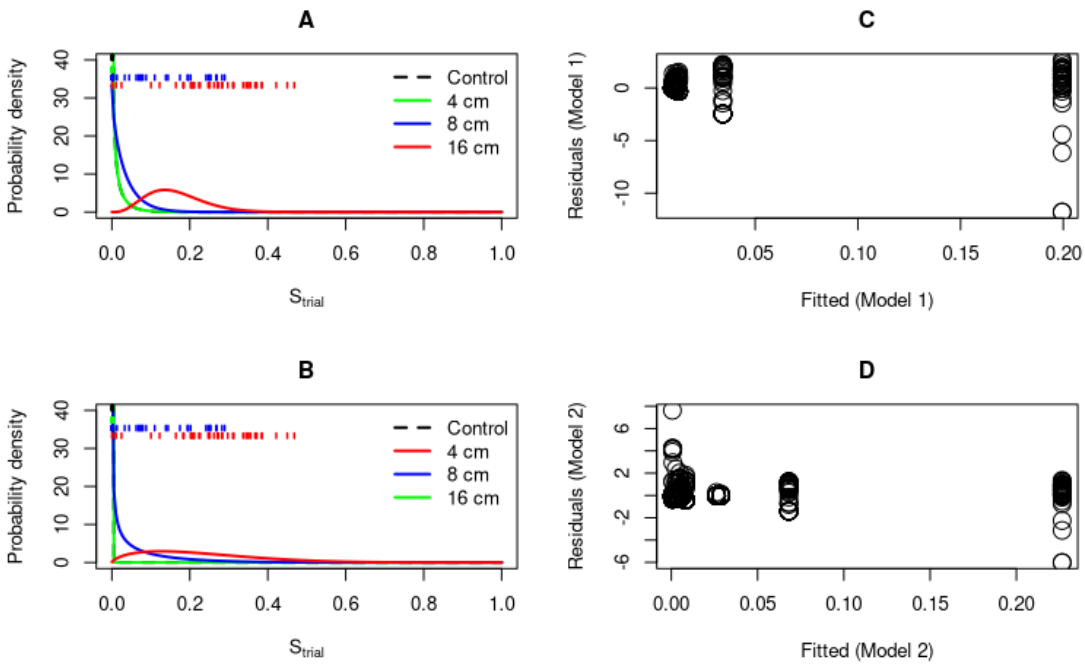

Figure S3. A-B) Probability densities of shimmering response to black stimuli against grey background predicted from the MLE parameters for Model 1 (A) and Model 2 (B). The *coloured ticks* (arranged vertically for clarity) are the original observations for S_{trial} (strength of shimmering) from the study. *'Control'* denotes the experimental condition where the string alone was moved, and 4 cm, 8 cm and 16 cm are the diameters

of the circular black stimuli. The *coloured lines* are density distributions of the shimmering response back-transformed for the sake of comparison with the original data. The spread of the predicted distributions fit the observed data better in the variable precision model (Model 2) compared to fixed precision model (Model 1). **(C-D) Standardised residuals against the fitted values for Model 1 (C) and Model 2 (D).** The spread of residuals in Model 1 is strongly related to the fitted values compared to Model 2 due to the single precision parameter in the former compared to variable precisions in the latter.

	Degrees of freedom	AIC	Model description
betaModelNull	2	-6651.213	Null model
betaModel1	25	-6967.681	Beta-regression with single precision
betaModel2	36	-12164.872	Beta-regression with variable precision
betaModel3	36	-12157.454	Beta regression with variable precision and bias correction
mixedModel1	26	-6987.611	Mixed-effects model

Table S1. Comparison of the four models (beta-regression and mixed-effects) to the null model

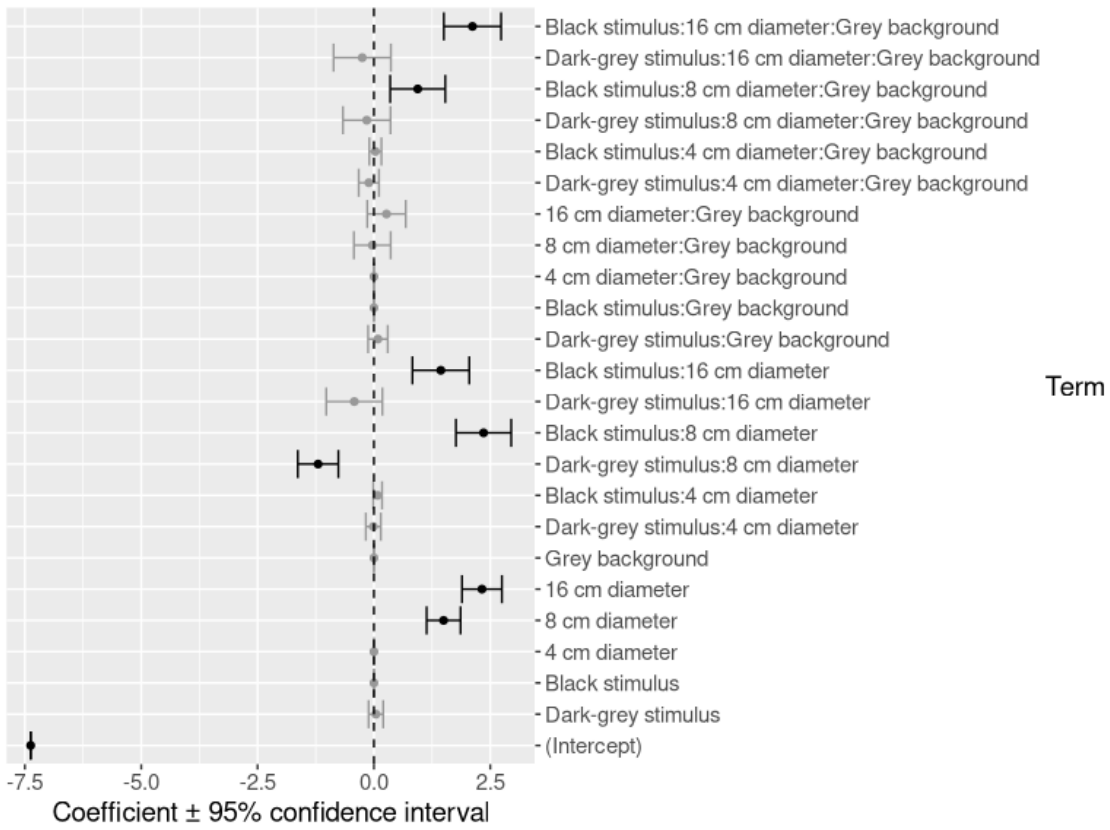

Figure S4. Estimated coefficients of the individual variables and the interaction terms for Model 2. The *filled circle* corresponds to the coefficient estimate and the *whiskers* represent the 95% confidence interval around it. The black *dot-whiskers* denote coefficients that contribute significantly to the model.

References

O'Carroll DC, Wiederman SD. Contrast sensitivity and the detection of moving patterns and features. *Philosophical Transactions of the Royal Society B: Biological Sciences. 2014 Feb 19;369(1636):20130043*

This document was generated from the [supplementary markdown file]. The details of the session and the packages used to generate this file are printed below

Session and packages info

```
##  setting  value
##  version  R version 4.1.2 (2021-11-01)
##  os       Fedora Linux 35 (Workstation Edition)
##  system   x86_64, linux-gnu
##  ui       X11
##  language en_GB
##  collate  en_IN.UTF-8
##  ctype    en_IN.UTF-8
##  tz       Asia/Kolkata
##  date     2022-02-07
##  pandoc   2.14.0.3 @ /usr/libexec/rstudio/bin/pandoc/ (via rmarkdown)
##             package ondiskversion         source
## betareg     betareg         3.1.4 CRAN (R 4.1.2)
## boot           boot        1.3.28 CRAN (R 4.1.2)
## cowplot     cowplot         1.1.1 CRAN (R 4.1.2)
## dplyr         dplyr         1.0.7 CRAN (R 4.1.1)
## ggplot2     ggplot2         3.3.5 CRAN (R 4.1.1)
## ggpubr       ggpubr         0.4.0 CRAN (R 4.1.2)
## glmmTMB     glmmTMB       1.1.2.3 CRAN (R 4.1.2)
## latex2exp latex2exp         0.5.0 CRAN (R 4.1.2)
## lubridate lubridate         1.8.0 CRAN (R 4.1.2)
## stringr     stringr         1.4.0 CRAN (R 4.1.2)
## tidyr         tidyr         1.1.4 CRAN (R 4.1.1)
```

The last section of the accompanying markdown file [sajesh_etal_2022_ESM.Rmd] contains the code for Fig 1b and Fig 2 in the main text. The plots can be generated by changing the value of the `include` *argument in the corresponding code-chunk to* `TRUE`